Palmitoylation of the K_{ATP} channel Kir6.2 subunit promotes channel opening by regulating PIP_2 sensitivity

Hua-Qian Yang[a], Wilnelly Martinez-Ortiz[b], JongIn Hwang[a], Xuexin Fan[c], Timothy J. Cardozo[b], and William A. Coetzee[a,b,d,1]

[a]Department of Pediatrics, New York University School of Medicine, New York, NY 10016; [b]Department of Biochemistry & Molecular Pharmacology, New York University School of Medicine, New York, NY 10016; [c]State Key Laboratory of Membrane Biology, College of Life Sciences, Peking University, Beijing 100871, China; and [d]Department of Neuroscience & Physiology, New York University School of Medicine, New York, NY 10016

Edited by Donald W. Hilgemann, University of Texas Southwestern Medical Center, Dallas, TX, and accepted by Editorial Board Member David E. Clapham March 17, 2020 (received for review October 15, 2019)

A physiological role for long-chain acyl-CoA esters to activate ATP-sensitive K^+ (K_{ATP}) channels is well established. Circulating palmitate is transported into cells and converted to palmitoyl-CoA, which is a substrate for palmitoylation. We found that palmitoyl-CoA, but not palmitic acid, activated the channel when applied acutely. We have altered the palmitoylation state by preincubating cells with micromolar concentrations of palmitic acid or by inhibiting protein thioesterases. With acyl-biotin exchange assays we found that Kir6.2, but not sulfonylurea receptor (SUR)1 or SUR2, was palmitoylated. These interventions increased the K_{ATP} channel mean patch current, increased the open time, and decreased the apparent sensitivity to ATP without affecting surface expression. Similar data were obtained in transfected cells, rat insulin-secreting INS-1 cells, and isolated cardiac myocytes. Kir6.2ΔC36, expressed without SUR, was also positively regulated by palmitoylation. Mutagenesis of Kir6.2 Cys^{166} prevented these effects. Clinical variants in *KCNJ11* that affect Cys^{166} had a similar gain-of-function phenotype, but was more pronounced. Molecular modeling studies suggested that palmitoyl-C166 and selected large hydrophobic mutations make direct hydrophobic contact with Kir6.2-bound PIP_2. Patch-clamp studies confirmed that palmitoylation of Kir6.2 at Cys^{166} enhanced the PIP_2 sensitivity of the channel. Physiological relevance is suggested since palmitoylation blunted the regulation of K_{ATP} channels by α1-adrenoreceptor stimulation. The Cys^{166} residue is conserved in some other Kir family members (Kir6.1 and Kir3, but not Kir2), which are also subject to regulated palmitoylation, suggesting a general mechanism to control the open state of certain Kir channels.

K_{ATP} channels | Kir6.2 | palmitoylation | PIP_2 | lipidation

On average, each protein-coding gene produces several unique proteins due to processes, such as alternative RNA splicing. The protein diversity is even higher when considering that the functional state can be significantly altered by post-translational modifications (PTM), which is such a fundamentally important aspect of protein regulation that ∼5% of the proteome are enzymes that perform more than 200 types of PTMs. These enzymes include kinases, phosphatases, transferases, and ligases that reversibly add and remove functional groups, proteins, lipids, or sugars at specific amino acid side chains. The best studied PTM involves phosphorylation of specific serine, threonine, tyrosine, or histidine residues. Lipid moieties can also posttranslationally be attached to specific amino acids (often referred to as lipidation). Examples include glycosyl phophatidylinositol anchoring, N-terminal myristoylation, S-myristoylation, and S-prenylation.

S-palmitoylation (also known as S-acylation) most commonly occurs when palmitoyl acyltransferases (PATs or DHHC enzymes) attach the C16 palmitoyl group from palmitoyl-CoA to the thiolate side chain of a cysteine residue (*SI Appendix*, Fig. S1). The reverse process, depalmitoylation, is mediated by two acyl-protein thioesterases, APT1 and APT2 (1), and recently characterized α/β-hydrolase domain-containing protein 17 members (2). The large, hydrophobic palmitate moiety can serve as a membrane lipid anchor in the target protein and the reversible nature of the reaction lends itself to dynamic changes in protein function and localization. Intracellular trafficking of Ras proteins was one of the first examples of a nontransmembrane protein that requires palmitoylation to reach the membrane (3). More recently, palmitoylation has been identified as a common mechanism that underlies the subcellular distribution and polarized trafficking of several proteins within cells (4, 5).

ATP-sensitive K^+ (K_{ATP}) channels open when the ADP:ATP ratio increases, thus coupling the intracellular energy metabolism to membrane excitability. The channel is composed of four inward rectifier K^+ (Kir6.x) channel subunits and four sulfonylurea receptor (SURx) subunits. The Kir6 and SUR subfamilies each has two members, respectively, Kir6.1 and Kir6.2, and SUR1 and SUR2, with the latter present as one of two splice variants (SUR2A or SUR2B) (6). The pancreatic β-cell K_{ATP} channel (Kir6.2/SUR1) has a key role in regulating the first phase of

Significance

Protein diversity is substantially increased by posttranslational modifications of amino acid residues. Lipidation is poorly characterized for ion channels. We found regulated S-palmitoylation to occur in certain K^+ channels (Kir3.4, Kir6.1, and Kir6.2). For Kir6.2, lipidation at Cys^{166} (or gene variants associated with diabetes) increases the channel open state. Experimental and molecular modeling studies show this due mainly to an increased sensitivity to PIP_2, which results in altered regulation of K_{ATP} channels by α1-adrenoceptor signaling in cardiomyocytes. Our data demonstrate complexity in the regulation of K_{ATP} channels by long-chain acyl-CoA esters, which can be both acute and direct, but also be mediated through regulated S-palmitoylation. Strategies aimed at regulating the palmitoylation state of K_{ATP} channels may represent new therapeutic opportunities.

Author contributions: H.-Q.Y., T.J.C., and W.A.C. designed research; H.-Q.Y., W.M.-O., J.H., X.F., and T.J.C. performed research; T.J.C. and W.A.C. contributed new reagents/analytic tools; H.-Q.Y., W.M.-O., X.F., T.J.C., and W.A.C. analyzed data; and H.-Q.Y., W.M.-O., T.J.C., and W.A.C. wrote the paper.

The authors declare no competing interest.

This article is a PNAS Direct Submission. D.W.H. is a guest editor invited by the Editorial Board.

[1]To whom correspondence may be addressed. Email: william.coetzee@nyu.edu.

This article contains supporting information online at https://www.pnas.org/lookup/suppl/doi:10.1073/pnas.1918088117/-/DCSupplemental.

First published April 24, 2020.

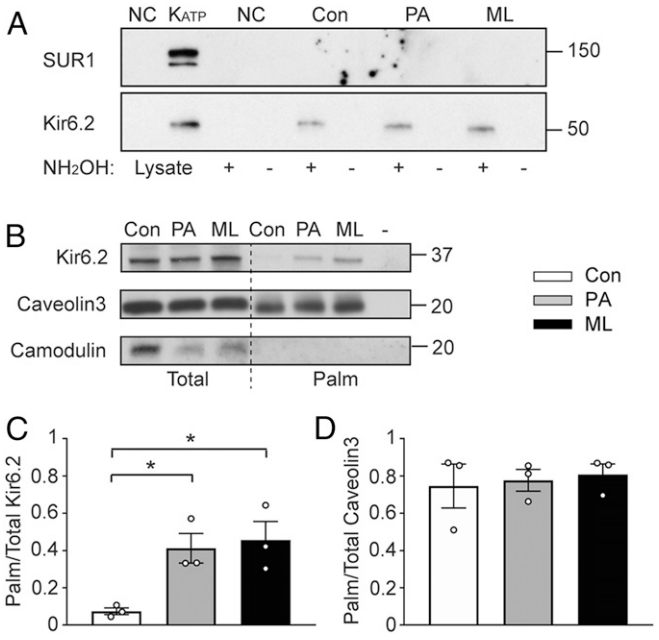

Fig. 1. K_{ATP} channels are palmitoylation targets. (*A*) The Kir6.2 but not SUR1 subunit is palmitoylated. Lysates of HEK-293 cells cotransfected with Kir6.2-myc/Flag-SUR1 were subjected to acyl-biotin exchange assays. Negative control reactions included untransfected cells (NC) or reactions without hydroxylamine (NH_2OH), in which the Cys-palmitoyl thioester linkages remain intact and cannot bind to biotin. Representative immunoblot of biotinylated proteins to detect SUR1 (with an anti-Flag antibody) or Kir6.2 (with an anti-myc antibody). The left two lanes are cell lystes. (*B*) Acyl-biotin exchange assay showed Kir6.2 subunit is palmitoylated in cultured rat adult cardiomyocytes, where "-" indicates a Tris-treated group as the negative experimental control and hydroxylamine was applied to control, PA, and ML groups. Caveolin3 and camodulin were used as positive and negative control, respectively. (*C*) Summary data of the stoichiometry of palmitoylated Kir6.2 to total Kir6.2. (*D*) Summary data of the stoichiometry of palmitoylated to total caveolin3. $n = 3$ blots per group. $^*P < 0.05$ vs. control determined by Dunnett's test following the ANOVA with repeated measures. Note that wild-type Kir6.2 migrates at ~37 kDa (e.g., in *B*), whereas Kir6.2-myc, which has six C-terminal myc epitopes, migrates at a ~50 kDa (e.g., in *A*).

insulin secretion and is the target of antidiabetic sulfonylureas, whereas the cardiac K_{ATP} channel (Kir6.2/SUR2A) regulates action potential adaptation with elevated heart rates and participates in cardioprotection (6).

Several ion channels have been described to be regulated by palmitoylation and the underlying mechanism often involves changes in channel subcellular trafficking, cell-surface expression, and clustering (7). Although K_{ATP} channels are targets of receptor signaling and PTM by protein phosphorylation (8), it is currently unknown how lipidation affects these channels or their regulation. Circulating palmitate is transported into cells and converted to palmitoyl-CoA, which can serve as the substrate for palmitoylation. A physiological role for long-chain acyl-CoA esters to activate K_{ATP} channels has been known for almost two decades (9, 10) and it is possible that some or all of these effects are due to S-palmitoylation. The purpose of these studies was therefore to investigate regulation of K_{ATP} channels by S-palmitoylation. We found that long-chain acyl-CoA and palmitoylation activate K_{ATP} channels in a similar manner, but through different mechanisms. The Cys^{166} residue of Kir6.2 is specifically modified by regulated palmitoylation, which leads to an increased open state without affecting trafficking effects or surface expression. Palmitoylation at this residue—or mutations at Cys^{166} that are associated with developmental delay, epilepsy, and neonatal diabetes—lead to molecular conformational changes that impact PIP_2 binding. These data point to K_{ATP} channel regulation by acyl-CoAs through semiredundant mechanisms. Strategies aimed at regulating the palmitoylation state of certain Kir channels (such as K_{ATP} channels) may represent new therapeutic opportunities for altering the channel open state, with clinical relevance in diabetes and heart disease.

Results

Kir6.2, but Not SUR, Is Palmitoylated. To examine regulated palmitoylation (i.e., altering the palmitoylation state when modulating the S-palmitoylation pathway), 2-bromo-palmitate (2-BP) is often employed as an S-palmitoylation inhibitor (11). However, our data show that 2-BP irreversibly blocks a variety of K^+ channels, including K_{ATP} channels, Kir2.1 and Kv4.3 (*SI Appendix*, Fig. S2), suggesting nonspecificity. We therefore employed alternative strategies to study regulated palmitoylation (*SI Appendix*, Fig. S1*B*). In one group of experiments, cells were preincubated with micromolar concentrations of C16:0 palmitic acid (PA), an intervention that promotes protein palmitoylation (12). In a complementary approach, depalmitoylation was prevented by inhibiting the thioesterases APT1 and APT2 with ML348 plus ML349 (ML) (13). To determine whether K_{ATP} channel subunits are S-palmitoylated, we performed acyl-biotin exchange assays to detect thioester-linked protein acyl-modifications in lysates of HEK-293 cells cotransfected with Kir6.2-myc and Flag-SUR1 (14). Kir6.2 displayed low basal levels of palmitoylation, which was significantly increased in cells preincubated with ML or PA. Regulated palmitoylation was not observed in negative control reactions or with SUR1 (Fig. 1*A*). Endogenous Kir6.2 in rat cardiomyocytes was also palmitoylated, and palmitoylation levels were increased by PA or ML (Fig. 1 *B* and *C*). Since both palmitate

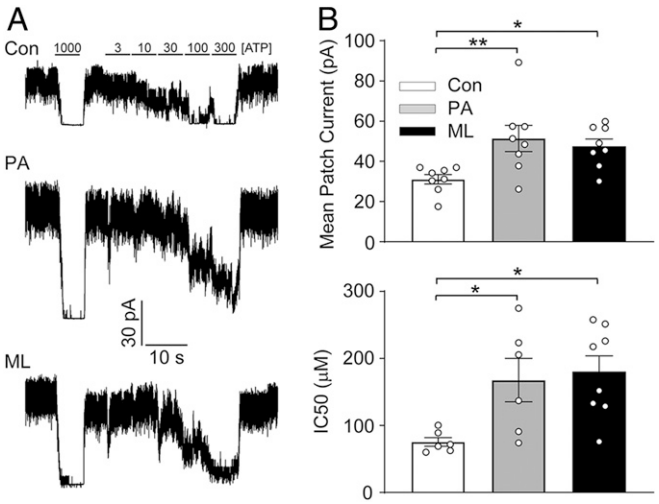

Fig. 2. Palmitoylation modulates endogenous K_{ATP} channels. (*A*) Representative inside-out current recordings obtained from cardiac myocytes in control, PA, and ML groups. ATP concentrations were switched as indicated. The mean patch current was recorded at a membrane potential of −80 mV and defined by the current component blocked by 1 mM ATP applied to the cytosolic face of the patch. The ATP-sensitivity of K_{ATP} channels was determined by plotting the K_{ATP} current (normalized to the maximum current) as a function of the cytosolic ATP concentration. Data from individual patches were subjected to curve fitting to a modified Boltzmann equation, yielding IC_{50} values for ATP inhibition. (*B*) Summary data of mean patch currents and IC_{50} of ATP-sensitivity for control, PA, and ML groups in cardiomyocytes. $n \geq 6$ patches in each group. $^*P < 0.05$, $^{**}P < 0.01$ vs. the control group determined by Dunnett's test following the ANOVA with repeated measures.

incubation and APT inhibition promoted palmitoylation, these data suggest that acyl-CoA synthetases and the acyl-transfereases are substrate-limited in these cellular assays. Caveolin, which is palmitoylated under basal conditions (15), was used as a positive control (Fig. 1 *B* and *D*). Calmodulin, which contains no cysteine residues and cannot be palmitoylated, was used as a negative control (Fig. 1*B*). These data demonstrate that the Kir6.2 subunit, but not SUR1, of the K_{ATP} channel is subject to regulated palmitoylation.

Palmitoylation Positively Regulates K_{ATP} Channels. To determine the functional consequences of palmitoylation, recordings of K_{ATP} channel activity were made using inside-out membrane patches in ATP-free conditions using cells that were preincubated with either PA or ML for 24 h. Both of these interventions led to a significant increase in the mean patch current of native K_{ATP} channels in isolated cardiac myocytes (Fig. 2), rat insulin-secreting INS-1 cells, and HEK-293 cells transfected with Kir6.2/SUR1 or Kir6.2/SUR2A subunit combinations (*SI Appendix*, Fig. S3 *A–C*). Moreover, higher ATP concentrations were needed to block channel activity, illustrated by a rightward shift of the ATP-sensitivity curves (Fig. 2*B* and *SI Appendix*, Fig. S3 *A–C*). We next used a truncated Kir6.2ΔC36 subunit, in which the endoplasmic reticulum retention motif is deleted to allow expression by itself (16), to determine if Kir6.2 can be palmitoylated in the absence of SURx. Patch-clamp data demonstrated that PA and ML increased the Kir6.2ΔC36 mean patch current and caused an apparent right-shift in the ATP-sensitivity curve (*SI Appendix*, Fig. S3*D*). Overall, these data demonstrate that K_{ATP} channel activity is positively regulated by S-palmitoylation and that palmitoylation of Kir6.2 is sufficient to recapitulate the functional effects observed with the full channel.

Micromolar concentrations of long-chain acyl-CoAs, such as oleoyl-CoA and palmitoyl-CoA, activate K_{ATP} channels functionally similar to regulated palmitoylation (e.g., in part by reducing the channel's ATP sensitivity) (9, 10, 17). The underlying mechanism has not been fully resolved. Our data (*SI Appendix*, Fig. S4) suggest that palmitoyl-CoA activates K_{ATP} channels independently of palmitoylation. Arguments include: 1) The rapid time course of activation (preincubation with palmitate is needed to activate K_{ATP} channels); 2) acute application of palmitoyl-CoA (1 μM), but not palmitate (10 μM), activates K_{ATP} channels; and 3) "spontaneous" nonenzymatic palmitoylation of cysteine residues may occur at millimolar concentrations of palmitoyl-CoA, but has not been demonstrated at micromolar concentrations. Moreover, two separate DHHC inhibitors, tunicamycin or cerinurien, failed to prevent activation of K_{ATP} channels by palmitoyl-CoA. Therefore, overall these data demonstrate a complexity of K_{ATP} regulation by low physiological concentrations of acyl-CoAs that depend both on palmitoylation and direct effects (possibly direct lipid effects). Subsequent experiments focus on mechanisms by which S-palmitoylation activates K_{ATP} channels.

Palmitoylation of Kir6.2 at Cys^{166} Regulates K_{ATP} Channel Function. We next determined the specific intracellular Kir6.2 cysteine residues that are S-palmitoylated. Kir6.2 has seven cysteine residues that are highly conserved across species, of which five are within intracellular domains (*SI Appendix*, Fig. S5). Bioinformatic analysis with CSS-Palm 3.0 predicted Cys^{166} as a likely candidate, which is further supported by the proximity of this residue to the inner membrane interface (18) (Fig. 3*A*). The active site of DHHC palmitoyl acyltransferases is positioned close to the membrane–cytosol interface (*SI Appendix*, Fig. S1) (19), and S-palmitoylation is therefore governed primarily by the proximity and accessibility of the transferase to target cysteine residues located near the membrane cytosolic face. Although the sequences surrounding the target cysteine are involved in recognition by specific DHHCs (20), a recent cysteine-scanning mutagenesis study demonstrated that S-palmitoylation can occur at any cysteine residue near the inner membrane interface, without an apparent need for an amino acid "consensus"

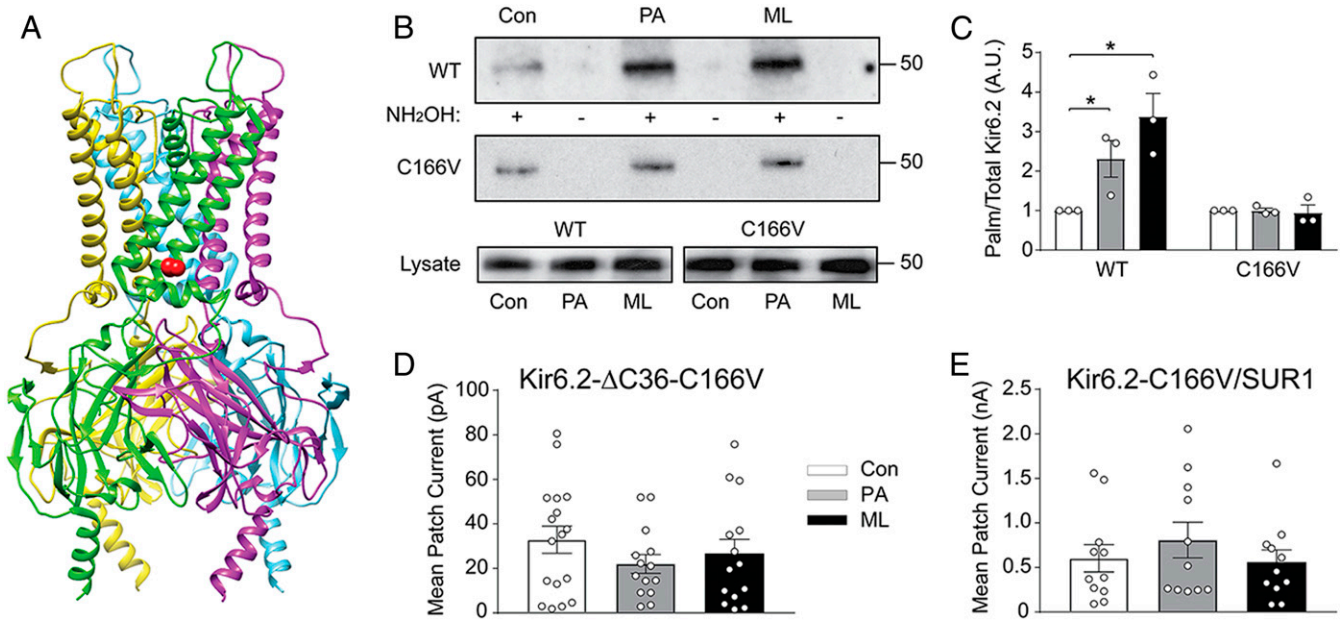

Fig. 3. Palmitoylation of Kir6.2 at position Cys^{166} regulates K_{ATP} channel function. (*A*) Side view of Kir6.2 tetramer, with one Cys^{166} highlighted in red (PDB ID code 6C3P). (*B*) Representative immunoblots of acyl-biotin exchange assay and (*C*) The normalized ratios of palmitoylated Kir6.2 to total Kir6.2 are shown for wild-type and C166V mutated K_{ATP} channels transfected in HEK-293 cells. $n = 3$ blots per group. $^*P < 0.05$ vs. control determined by Dunnett's test following the ANOVA with repeated measures. Summary data of mean patch currents for Kir6.2-ΔC36 (*D*) and Kir6.2/SUR1 (*E*) channels carrying C166V mutation. $n \geq 11$ patches in each group.

sequence (21). The same study demonstrated that palmitoylation can occur up to 8 Å (e.g., approximately five to six residues/1.5 turn of an α-helix) into the membrane (21), most likely due to the ability of DHHC enzymes to locally reshape the membrane (22). Several of the ion channel palmitoylation sites identified to date are in fact near a membrane interface (7). Attempts have previously been made to explore the biochemical nature of residue Cys^{166} as a modifier of channel gating (23). Mutagenesis of Cys^{166} in Kir6.2 to leucine, serine, threonine, alanine, methionine, or phenylalanine all greatly increase the open state of Kir6.2-ΔC26 channels, whereas substitution with a valine lacked this effect. To avoid confounding effects on gating in data interpretation, we generated a C166V mutation, which prevented palmitoylation of Kir6.2 by ML or PA (Fig. 3 *B* and *C*), thus demonstrating that Kir6.2 Cys^{166} is the major regulated palmitoylated site of K_{ATP} channels.

We performed patch clamping to verify the functional relevance of Cys^{166}. Similar to the previous report (23), the C166V mutation by itself did not significantly affect the mean patch current or ATP sensitivity, either when expressed by itself (Kir6.2-C166VΔC36) or with SUR1 (*SI Appendix*, Fig. S6). The Kir6.2-C166VΔC36 or Kir6.2-C166V/SUR1 channels, however, became unresponsive to PA or ML (Fig. 3 *D* and *E*). These data demonstrate that Kir6.2 Cys^{166} is the sole residue that mediates the positive regulation of K_{ATP} channels by palmitoylation.

Palmitoylation Does Not Increase the K_{ATP} Channel Surface Expression. The hydrophobic nature of the palmitate moiety can anchor target proteins to specific membranes or subcellular compartments (4, 5). Indeed, the surface expression of several G protein-coupled receptors, ion channels, and transporters is promoted by palmitoylation (7). To investigate whether the increased mean patch K_{ATP} channel current is due to enhanced membrane targeting, we biochemically assessed the surface expression of K_{ATP} channels. As in our previous study (24), we performed surface biotinylation of Kir6.2 with an extracellular Avi tag (Avi-Kir6.2), which functions and traffics similar to wild-type Kir6.2. The Avi-Kir6.2/SUR1 channels were expressed in HEK-293 cells and we confirmed that they are palmitoylated similarly to the wild-type channel (*SI Appendix*, Fig. S7*A*). Pretreatment with PA or ML affected neither the total Kir6.2 protein level nor the surface expression of K_{ATP} channels (*SI Appendix*, Fig. S7*B*). Thus, it appears likely that palmitoylation regulates the K_{ATP} channel open probability.

Palmitoylation Positively Regulates the K_{ATP} Channel Open Probability. To investigate whether palmitoylation affects K_{ATP} channel dwell kinetics, we studied Kir6.2ΔC36 in the absence of SUR in inside-out membrane patches. We found the unitary current amplitude to be unaffected by PA or ML (*SI Appendix*, Fig. S8). Event detection and dwell-time kinetic analysis was performed with recordings obtained immediately after patch excision to avoid confounding effects of rundown. Open-time histograms were subjected to curve fitting with a single exponential function and closed-time histograms with a sum of three exponential functions. This analysis showed that the mean open times were unchanged by PA or ML. Similarly, the short and intermediate closed states were unaffected. In contrast, the time constant of the longest closed state, which represents the interburst closed time, was significantly reduced by PA and ML (Table 1 and *SI Appendix*, Fig. S8). To examine bursting behavior, we fitted the burst duration distribution with a sum of two exponential functions (*SI Appendix*, Fig. S8). The interburst interval was significantly reduced (Table 2), demonstrating that bursting occurred more frequently with PA or ML treatment. Thus, palmitoylation destabilizes the closed state, leading to an overall increase in K_{ATP} channel open probability. PA or ML treatment also led to an increased open probability of endogenous K_{ATP} channels in INS-1 cells, without having an effect on the unitary current amplitude (*SI Appendix*, Fig. S9).

Palmitoylation of Cys^{166} Sensitizes the K_{ATP} Channel to PIP_2. PIP_2 promotes the transition of the K_{ATP} channel from closed state to open state. Since the palmitoylated K_{ATP} channel had an increased open probability and reduced ATP sensitivity, we next tested the hypothesis that palmitoylation of Cys^{166} affects K_{ATP} channel PIP_2 sensitivity. Ca^{2+}-induced rundown of K_{ATP} channels in excised patches occurs from the hydrolysis of PIP_2 by activation of an endogenous Ca^{2+}-dependent phospholipase C (PLC) (25, 26) and can be partially restored by PIP_2-diC8 (26). We found that PIP_2 more effectively reactivated K_{ATP} channel current after Ca^{2+}-induced rundown in patches from ventricular myocytes when preincubated with ML or PA (Fig. 4 *A* and *B*). Similar data were obtained with wild-type Kir6.2/SUR2A, but not with Kir6.2-C166V/SUR2A (Fig. 4 *C* and *D*). These data demonstrate that at any given PIP_2 level, palmitoylation of Kir6.2 at Cys^{166} increased the open probability of both transfected and native K_{ATP} channels.

Physiological Relevance: Palmitoylation Blunts α1-Adrenoreceptor Regulation of K_{ATP} Channels. Membrane PIP_2 levels, a key regulator of K_{ATP} channel activity (25, 27, 28), are determined by a balance between PLC-mediated hydrolysis and replenishment by PI kinases (29). Signaling of several hormone receptors converges on regulating PLC activity, including muscarinic, α1-adrenergic (AR), endothelin, and angiotensin receptors (30), which all inhibit Kir channels (31–33). We previously demonstrated that α1-AR stimulation inhibits cardiac K_{ATP} channel activity by depleting membrane PIP_2 levels (34), which we directly measured with a fluorescent PIP_2 reporter protein (PLCδ PH-GFP). Since lipidation sensitizes the K_{ATP} channel to PIP_2, we hypothesized that lipidated channels will become less responsive to α1-AR–mediated PIP_2 hydrolysis. As expected, the α1-adrenoreceptor agonist methoxamine (MTX; 300 μM) reversibly inhibited pinacidil-evoked whole-cell K_{ATP} current in cardiac ventricular myocytes (34). The degree of MTX-induced inhibition was significantly reduced by PA or ML (Fig. 5*B*). This finding could be recapitulated when using HEK-293 cells cotransfected with Kir6.2, SUR2A, and α1-adrenoreceptor cDNAs (Fig. 5*C*). Notably, the lipidation response was lost in the palmitoylation-negative Kir6.2-C166V channel (Fig. 5 *A* and *C*), demonstrating that the change of K_{ATP} channel sensitivity to membrane PIP_2 is entirely attributed to an action on Kir6.2-C166.

KCNJ11 Variants at Cys^{166} Associated with Genetic Disorders also Regulate K_{ATP} Channel Open Probability. Variants in *KCNJ11* and *ABCC8* (the genes coding for Kir6.2 and SUR1) are commonly associated with diabetes (35). Interestingly, there are two *KCNJ11* variants (p.Cys166Phe and p.Cys166Tyr) at the palmitoylated Cys^{166} residue associated with cases of developmental delay, epilepsy, and neonatal diabetes (ClinVar accession numbers: VCV000021197.1 and VCV000008679.1). Kir6.2-C166F-ΔC26 has previously been shown to increase the K_{ATP} channel open probability (23) but Kir6.2-C166Y has not been characterized. Here we functionally characterized both mutants in HEK-293 cells when coexpressed with SUR1. Each of the variants reduced the mean patch current (Fig. 6*A*), but strongly mitigated the apparent sensitivity of the channel to intracellular ATP, with IC_{50} values increasing by two orders-of-magnitude (Fig. 6*B*), which overall represents a gain-of-function and potentially clinically relevant phenotype. As expected, both mutants were insensitive to interventions that promote palmitoylation (*SI Appendix*, Fig. S10). Moreover, Ca^{2+}-dependent PIP_2 depletion led to significant "rundown" of wild-type Kir6.2/SUR1 channels, which could be partially restored by

Table 1. Single channel kinetics of K_{ATP} channels

	τ_{Open} (ms)	τ_{Close1} (ms)	τ_{Close2} (ms)	τ_{Close3} (ms)	α_{Close1}	α_{Close2}	α_{Close3}	P_o
Control	0.99 ± 0.02	0.37 ± 0.01	46.6 ± 6.6	1,043 ± 141	0.56 ± 0.01	0.41 ± 0.01	0.02 ± 0.003	0.02 ± 0.002
PA	0.95 ± 0.02	0.39 ± 0.01	38.9 ± 3.8	583.1 ± 122*	0.55 ± 0.03	0.43 ± 0.03	0.01 ± 0.005	0.05 ± 0.007*
ML	1.05 ± 0.07	0.41 ± 0.01	28.5 ± 3.8	425.5 ± 145*	0.65 ± 0.05	0.32 ± 0.04	0.01 ± 0.005	0.05 ± 0.007*

Summary of data from experiments depicted in *SI Appendix*, Fig. S8. PA and ML refer to cells preincubated for 24 h, respectively, with 10 μM palmitic acid or with a combination of 10 μM ML348 and 10 μM ML349, $n \geq 4$ patches in each group.
*$P < 0.05$ vs. control determined by Dunnett's test following the ANOVA with repeated measures.

PIP2-diC8 (Fig. 6*C*). In contrast, Kir6.2-C166Y/SUR1 channels were relatively insensitive to Ca^{2+} under the same experimental conditions, but could be blocked by the nonspecific Kir channel pore blocker, Ba^{2+} (Fig. 6 *C* and *D*). These data demonstrate that the open state of Kir6.2-C166Y can be maintained at significantly lower PIP_2 concentrations compared to wild-type.

The Palmitoyl Moiety of Palmitoyl-Cys^{166} Makes Direct Hydrophobic Contact with PIP_2 in a 3D Model, Potentially Promoting the K_{ATP} Channel Open State. An X-ray crystallographic structure of mouse Kir3.1 (PDB ID code 3SYQ; 3.44 Å) bound to PIP_2 in the channel's open conformation and a low-resolution cryogenic electron microscopy (cryo-EM)-derived structural model of Kir6.2 in its closed, ATP-bound conformation (PDB ID code 6C3P; 5.6 Å) have been reported (36, 37). We recently published a new method to model ion channels to maximal atomic-detail accuracy from low-resolution X-ray and cryo-EM data (38), which enables accurate 3D modeling of ion channels. With these structure coordinates as templates, we generated 3D models of the Kir6.2-palmitoyl-C166, Kir6.2-C166V, Kir6.2-C166F, and Kir6.2-C166Y homotetramers in both the open and closed states. In both states, the palmitoyl moiety of palmitoyl-C166 of one monomer extends directly toward the hydrophobic ether moieties of the C8-PIP_2 ligand (present in the 3SYQ high-resolution structure) bound to an adjacent monomer, with the open state placing the palmitoyl, Phe, or Tyr, slightly closer (Fig. 7). The distance is just great enough that the large hydrophobic palmitoyl, Phe, or Tyr, can span the solvent cavity between the Cys^{166} peptide backbone and the PIP_2 molecular surface, but the smaller Val cannot. As hydrophobic contacts are the driving force of binding affinity, this structural model predicts increased PIP_2 sensitivity with Kir6.2-palmitoyl-C166, Kir6.2-C166F, and Kir6.2-C166Y, since a new hydrophobic contact with the PIP_2 ligand is made with these modifications, but absence of increased binding with Kir6.2-C166V. Since Cys^{166} is at the cytosolic end of the inner helix of one monomer and PIP_2 is at the cytosolic end of the outer helix of the adjacent monomer, the model also predicts that palmitoyl/Phe/Tyr binding to PIP_2 brings these two helices closer together, which, from inspection of the structure, is predicted to straighten them slightly and opening the connected, adjacent inner helix gate.

Palmitoylation of Other Kir Channels. Multiple sequence alignment of human Kir channels show that the Kir6.2-C166 is conserved in Kir6.1 and Kir3.x, but not in other Kir channels (Fig. 8*A*). We therefore tested if this specific cysteine is a conserved palmitoylation site in these Kir channels. HEK-293 cells were transfected with Kir2.1, Kir6.1/SUR2A, or Kir3.4 and subjected to an acyl-biotin exchange assay, which demonstrated that (as with Kir6.2) palmitoylation was induced by PA for Kir6.1 and Kir3.4, but not with Kir2.1, which lacks a cysteine residue at the corresponding site (Fig. 8*B*). When introducing a cysteine at this position in Kir2.1 (Kir2.1-A178C), palmitoylation can be forced, which demonstrates the relevance of the cysteine residue in proximity to the inner membrane interface for lipidation to occur.

Discussion

Our data demonstrate that physiologically relevant low concentrations of long-chain acyl-CoAs and interventions that promote palmitoylation similarly increase K_{ATP} channel activity by causing an apparent decrease in the channel's sensitivity to ATP. There are at least two underlying mechanisms, with long-chain acyl-CoAs having rapid (and possibly direct) effects, whereas enzymatic regulation of the K_{ATP} channel by S-palmitoylation occurs over a slower time scale. Our studies have focused on studying the mechanism of the latter and we show that S-palmitoylation occurs at residue Cys^{166} of Kir6.2, which is sufficient for functional activation. The K_{ATP} channel surface expression is unaffected by palmitoylation, but the dwell times are significantly altered as to destabilize the channel's closed state. Molecular modeling predicts an underlying mechanism of a new tertiary structural contact being formed between the C166 position and PIP_2, which is hypothesized to result in enhanced PIP_2 binding. The new tertiary contact, in turn, is predicted to alter helical packing around the pore to favor the open state. Enhanced PIP_2 sensitivity, consistent with this predicted model, was demonstrated by independent patch clamp studies. Disease-causing mutations of Cys^{166} may promote channel opening by a similar mechanism. A wider screen of Kir channels showed that a specific cysteine near the membrane–cytosol interface beneath the second transmembrane domain is a conserved palmitoylation site in several Kir channels.

Palmitoylation as a Regulator of Channel Surface Density. Lipid modifications of proteins can increase membrane targeting since the hydrophobic moiety can serve as a membrane anchor. Ras, for example, requires palmitoylation to reach the membrane (3). Palmitoylation as a mechanism for protein delivery is emerging as a common process for membrane targeting, subcellular distribution, and polarized trafficking within cells (4, 5). Palmitoylation also increases the subcellular trafficking, cell-surface

Table 2. Burst analysis of K_{ATP} channels

	τ_{burst1} (ms)	τ_{burst2} (ms)	α_{burst1}	α_{burst2}	$T_{interburst}$ (ms)
Control	2.15 ± 0.64	189 ± 17.0	0.19 ± 0.01	0.80 ± 0.01	409 ± 25.5
PA	1.35 ± 0.28	232 ± 48.4	0.22 ± 0.03	0.77 ± 0.03	279 ± 43.4*
ML	0.89 ± 0.06	175 ± 55.2	0.19 ± 0.03	0.80 ± 0.03	189 ± 39.1*

PA and ML refers to cells preincubated for 24 h, respectively, with 10 μM palmitic acid or with a combination of 10 μM ML348 and 10 μM ML349, $n \geq 4$ patches in each group.
*$P < 0.05$ vs. control determined by Dunnett's test following the ANOVA with repeated measures.

PHYSIOLOGY

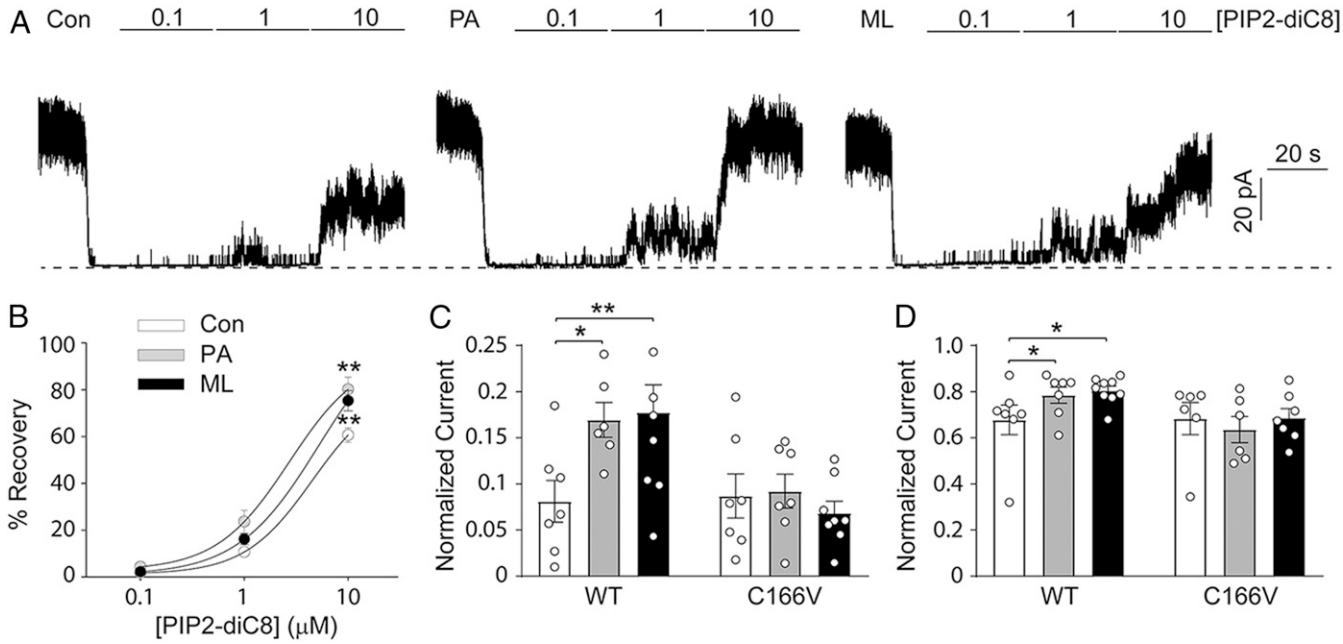

Fig. 4. Palmitoylation enhances K_{ATP} channel PIP_2 sensitivity. (*A*) Representative inside-out current recordings obtained from cardiomyocytes in control, PA, and ML groups. PIP_2–diC8 concentrations were switched as indicated right after Ca^{2+} induced rundown. (*B*) Fractional currents (recovered currents normalized by the baseline current) for control, PA, and ML groups in cardiomyocytes was plotted as a function of PIP_2–diC8 concentration and subjected to curve fitting to a modified Hill equation. Summary data of fractional currents for 1 μM (*C*) and 10 μM (*D*) PIP_2–diC8 in HEK-293 cells transfected with either wild-type or C166V mutated K_{ATP} channels. $n \geq 6$ patches in each group. $^*P < 0.05$, $^{**}P < 0.01$ vs. control determined by Dunnett's test following the ANOVA with repeated measures.

expression, and clustering of several ion channels (7). In contrast, we have not observed changes in K_{ATP} channel surface membrane expression by palmitoylation when measured with surface biotinylation assays. Moreover, there were no significant alterations in the subcellular localization of K_{ATP} channels in cardiac ventricular myocytes (*SI Appendix*, Fig. S11). The effects of palmitoylation on K_{ATP} channels therefore appear to be primarily due to changes in gating.

Palmitoylation as a Regulator of Channel Gating. Palmitoylation has not generally been shown to be a major regulatory mechanism of the intrinsic activity or as a gating modifier of ion channels. An exception worth noting is that Kv1.1 was shown to be palmitoylated at residue Cys^{243} under basal conditions (39). Mutagenesis of this residue (C243A) reduces current density (consistent with trafficking defects) and also caused a 20-mV hyperpolarizing shift in the voltage-dependence of activation, but is not clear whether this effect was caused by eliminating effects of palmitoylation or whether this result occurred because of the mutation. Another example is that incubation of neonatal cardiomyocytes with palmitate causes a relatively small depolarizing shift (by ~7 mV) of the steady-state inactivation curve of the Na^+ current with an increase in the "late" current, without affecting the I_{Na} inactivation rates or Na^+ current amplitude (12). 2-BP had much more pronounced effects in the latter study, but this finding should be interpreted with caution since we found this compound to rapidly (within seconds) and irreversibly lead to inactivation of several classes of K^+ channels, including the inward rectifying Kir2.1 channel, which is not palmitoylated. Moreover, these effects of 2-BP were likely not related to palmitoylation since

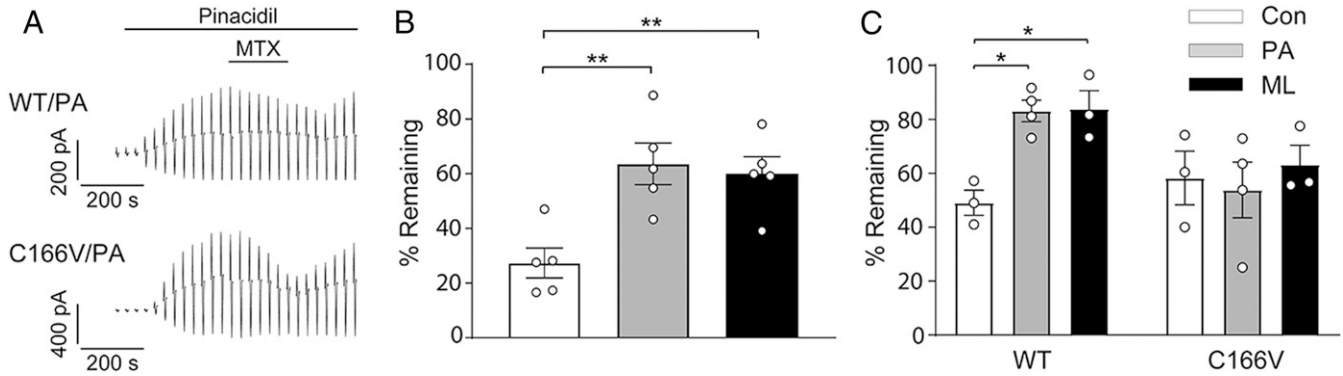

Fig. 5. Palmitoylation desensitizes K_{ATP} channel to membrane PIP_2 change. (*A*) Representative whole-cell K_{ATP} current recordings from PA treated HEK-293 cells transfected with α1-adrenoreceptor and either wild-type or C166V mutated K_{ATP} channels (Kir6.2/SUR2A). Pinacidil and MTX are applied as indicated. Percentage of remaining (minimum current recorded at the presence of MTX normalized by the maximum current with pinacidil only) for control, PA, and ML groups in cardiomyocytes (*B*) and HEK-293 cells transfected with either wild-type or C166V mutated K_{ATP} channels (*C*). $n \geq 3$ patches in each group. $^*P < 0.05$, $^{**}P < 0.01$ vs. control determined by Dunnett's test following the ANOVA with repeated measures.

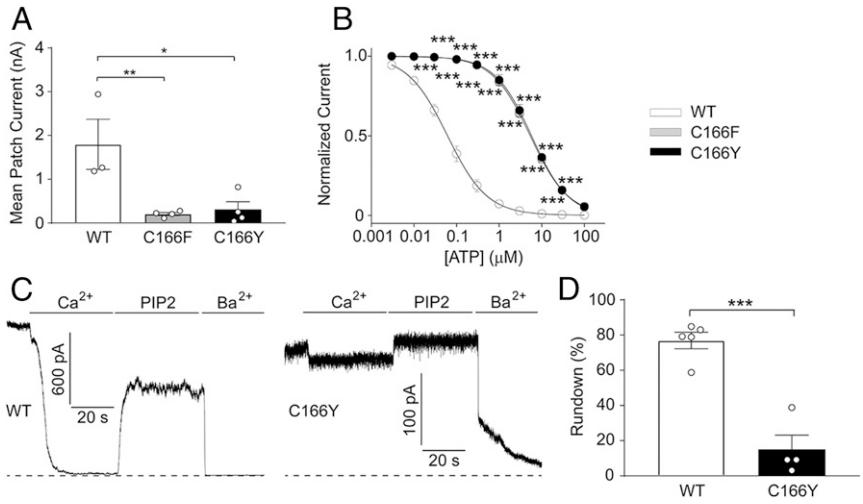

Fig. 6. *KCNJ11* variants at Cys^{166} associated with genetic disorders also regulate K_{ATP} channel activity. (*A*) Summary data of mean patch currents for wild-type K_{ATP} channel and channels carrying C166F and C166Y mutations. (*B*) Fractional currents (normalized by the mean patch current in the absence of ATP) were plotted as a function of ATP concentration and subjected to curve fitting to a modified Hill equation for wild-type K_{ATP} channel and channels carrying C166F and C166Y mutations. $n \geq 3$ patches in each group. $^*P < 0.05$, $^{**}P < 0.01$, $^{***}P < 0.005$ vs. wild-type determined by Dunnett's test following the ANOVA with repeated measures. (*C*) Representative inside-out current recordings from wild-type and C166Y K_{ATP} channels, perfused with 100 μM Ca^{2+}, 10 μM PIP_2-diC8 and 1 mM Ba^{2+}. Dashed lines indicate closed state. (*D*) Summarized data of percentage of Ca^{2+}-induced rundown for wild-type and C166Y K_{ATP} channels. $n \geq 4$ patches in each group. $^{***}P < 0.005$ vs. wild-type determined by unpaired *t* test.

they could not be reversed by palmitate. Overall, the published literature therefore does not make a strong case for palmitoylation as a significant regulator of channel gating. In contrast, our present data demonstrate that palmitoylation significantly increases the stability of the open state of the K_{ATP} channel, with increased open probability and reduced ATP sensitivity, which leads to overall increase in channel activity. It is not clear whether the reduced ATP sensitivity represents a real change (e.g., in ATP binding affinity) or whether this is an

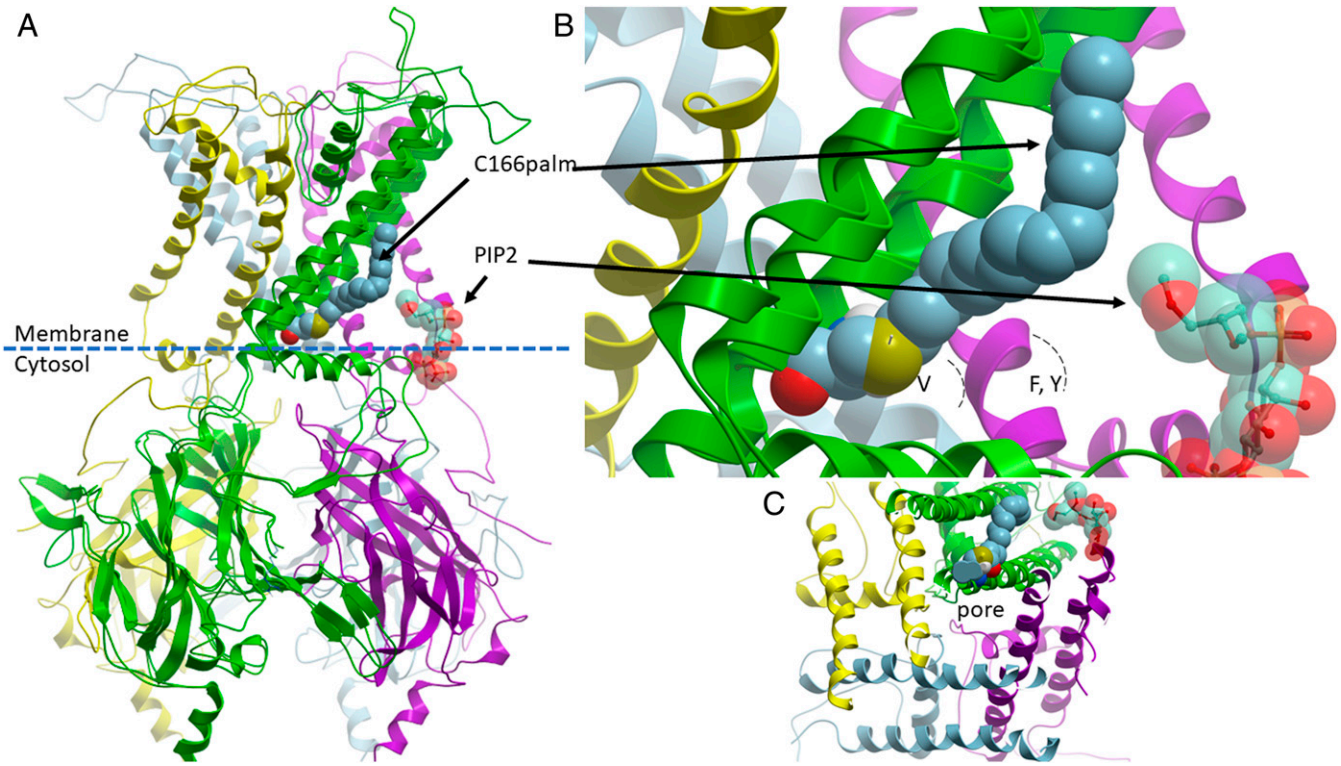

Fig. 7. C166-bound palmitate chain can directly contact PIP_2. (*A*) Side view of the Kir6.2 pore-forming tetramer (each monomer is displayed in ribbon depiction in a different color: Purple, yellow, green and gray) in the open conformation (PDB ID code 3SYQ) with Cys^{166} from the green monomer palmitoylated and the PIP_2 binding site from the purple monomer displayed. The carbon chain of palmitoyl-C166 contacts the hydrophobic ether moeities of PIP_2. A model of the green monomer based on the closed state (PDB ID code 63CP) is superimposed. (*B*) Magnified same view as in *A* of the palmitoyl-C166 interaction with PIP_2, showing the expected projections of C166F, Y, and V. (*C*) View perpendicular to the membrane from the intracellular face of the pore of Kir6.2 showing the proximity of the inner helix gate to the palmitoyl-C166 interaction with PIP_2 at the cytosolic membrane interface.

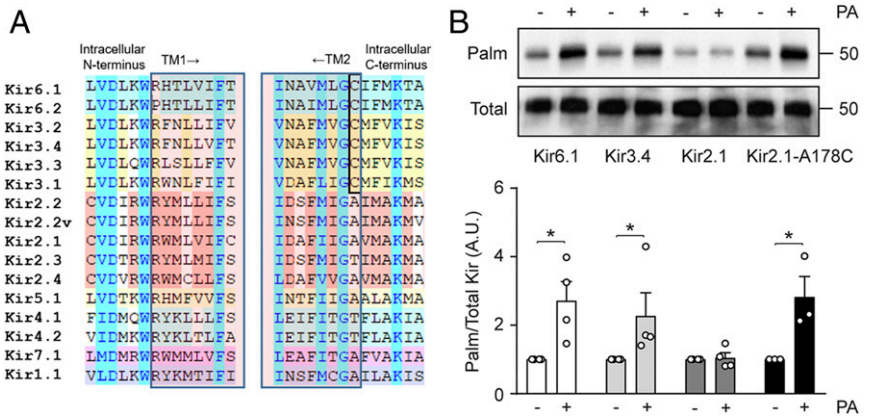

Fig. 8. Conserved palmitoylation site across Kir channels. (*A*) Of the human inward rectifier K^+ channel (Kir) subunits, only the Kir3.x and Kir6.x subfamilies have a conserved cysteine residue at the inner membrane interface (dark box). Shown are sequence alignments of Kirx.x subunits of selected regions that span the inner membrane interface. The light blue boxes, respectively, indicate the start and end of the M1 and M2 transmembrane helixes. Shading is by group conservation. The boxed Cys is the putative palmitoylation site. (*B*) Representative acyl-biotin exchange assay immunoblots and the ratios of palmitoylated to total Kir subunits for Kir6.1, Kir3.4, Kir2.1, and Kir2.1-A178C. $n \geq 3$ blots per group. $^*P < 0.05$ vs. control determined by unpaired *t* test.

apparent change resulting from the fact that ATP binds to the channel in the closed state, which is less readily available after palmitoylation.

Kir6.2 Residue Cys^{166} as a Regulator of Channel Function. A variety of approaches led us to conclude that Cys^{166} is the key residue that is palmitoylated and responsible for transduction of functional alterations of the K_{ATP} channel. First, Kir6.2 currents are increased regardless of whether it is expressed by itself (Kir6.2-ΔC36) or in the presence of SUR1 or SUR2A. Using bioinformatics, acyl-biotin exchange assay, and mutagenesis, we have established that Cys^{166} is a palmitoylation target. Mutagenesis of Cys^{166} eliminates the functional effects of palmitoylation, even when Kir6.2 is coexpressed with SURx subunits, demonstrating the importance of this residue and the absence of functionally relevant palmitoylation sites in SURx. Attempts have previously been made to explore the biochemical nature of residue Cys^{166} as a modifier of channel-gating (23). Mutagenesis of Cys^{166} in Kir6.2 to leucine, serine, threonine, alanine, methionine, or phenylalanine were shown all to greatly increase the open state of Kir6.2-ΔC26 channels, whereas substitution with a valine lacked this effect. In the present study, we found that a phenylalanine or a tyrosine residue at the 166 position also greatly increases K_{ATP} channel open probability. A palmitate group (which also increases channel activity) adds bulk and hydrophobicity but does not affect charge. Overall, there is no consistent side-chain property of the residue at position 166 that can adequately explain the effect on channel kinetics. We therefore turned to molecular modeling in an attempt to clarify the mechanisms by which modification of Cys^{166} alters gating.

For hERG and Ca^{2+}-activated K^+ channels, gating occurs at the selectivity filter. For many eukaryotic Kv and Kir channels, however, gating occurs near the intracellular membrane interface at the helix bundle crossing (HBC) (*SI Appendix*, Fig. S12). The restriction point is mediated by a conserved phenylalanine, F168 or F181, respectively, for Kir6.2 or Kir3.1 (40) (*SI Appendix*, Fig. S12), and only a slight shift of the M2 helix distinguishes the closed and open conformations. Kir6.2-C166 is located in the hydrophobic protein core in close proximity to this gate and modification of the cysteine at Kir6.2-C166 by mutagenesis or palmitoylation can potentially affect HBC gating by a variety of hypothesized mechanisms. 1) Abrogating disulfide bonds at this cysteine: This can largely be ruled out since there are no other cysteines adjacent to Cys^{166} (*SI Appendix*, Fig. S13). 2) Disrupt the tight packing of Cys^{166} with other hydrophobic residues in the protein core and lead to conformational changes and repositioning of the HBC gate due to protein instability. 3) Other, as yet undiscovered, mechanisms: Palmitoylation has been reported to modify the relationship of membrane proteins with PIP_2 (41, 42). Our 3D model reveals a clear mechanism by which modification of Cys^{166} could hypothetically lead to repacking of helices lining the pore by way of increased contact with PIP_2. Such a contact is also predicted to result in increased PIP_2 binding, which may modulate the sensitivity of the channel to this activator (43). In contrast, C166V had no such effect, consistent with its lack of functional effects in the patch-clamp studies. The computational approaches yield predictions that can be tested experimentally, and we have shown that (as predicted), the channel's sensitivity to PIP_2 and to α1-adrenoreceptor stimulation is significantly affected by palmitoylation or side-chain alterations at Cys^{166}. These data highlight a key role for Kir6.2-C166, lipidation of this residue or generic variants affecting this residue, in human health and disease.

Physiological and Pathophysiological Relevance. Regulation of K_{ATP} channels by acyl-CoAs is well established. For example, K_{ATP} channel activation has been reported by intracellular accumulation of acyl-CoA, which occurs in high glucose conditions and in response to inhibition of acyl-carnitine transferase by etomoxir (9). Our data show that in addition to the acute regulation of the channel by acyl-CoAs, enzymatic regulated S-palmitoylation is an additional mechanism that mediates the function of long-chain acyl-CoAs. The roles of palmitoylation in human health and disease remains incompletely characterized. We show here that palmitoylation of Kir6.2 modulates the sensitivity of K_{ATP} channels to α1-adrenoreceptor stimulation. A potential role of palmitoylation may also exist during reoxygenation following an anoxic period in cardiomyocytes, which causes massive endocytosis that coincides with activation of K_{ATP} channels (44). Modification of the Kir6.2-C166 palmitoylation site is also associated with insulin secretion disorders and Cantú syndrome. Genetic variants in both *KCNJ11* and *ABCC8* (the genes that, respectively, encode the Kir6.2 and SUR1 subunits) are associated with several types of insulin secretion disorders and diabetes (35). Interestingly, at the Cys^{166} residue that we have identified as a palmitoylation target, two *KCNJ11* variants have been reported to be associated with developmental delay, epilepsy and neonatal diabetes. The missense variants, NM_000525.3(KCNJ11):c.497G > T (p.Cys166Phe) and NM_000525.3(KCNJ11):c.497G > A (p.Cys166Tyr), are both predicted to be pathogenic by American College of Medical

Genetics standards, but both lacked assertion criteria. These variants are absent in the GenomeAd database, which represents over 200,000 alleles. Given their potential pathogenicity and that these variants are novel, we characterized them functionally. Patch-clamp studies showed that both variants caused a reduction in K_{ATP} channel density, which was offset by an ~100-fold reduction of the ATP sensitivity of the channel.

These data suggest an overall gain-of-function phenotype since significant K_{ATP} currents can be present even when the intracellular ATP levels are high. Since palmitoylation of Cys^{166} also elevates K_{ATP} channel opening, it is possible that this lipid posttranslational modification may be involved in inhibiting insulin secretion. This argument is supported by the finding that chronic palmitate exposure decreases glucose-induced insulin secretion from pancreatic islets (45). Even though the latter studies attributed the effect to alteration in fatty acid oxidation, our data suggest a potential contribution by palmitoylation, which may represent a new therapeutic target. Multiple sequence alignment of human Kir channels show that the Kir6.2-C166 is also conserved in Kir6.1 (Cys^{176}), and we demonstrated that Kir6.1 is also a palmitoylation target (Fig. 8). Interestingly, a mutation at the conserved cysteine (Kir6.1-C176S), resulting in gain of K_{ATP} channel function, has been characterized to induce Cantú syndrome (46), which may indicate a potential role of palmitoylation in this syndrome.

Limitations. So far, there are no specific antibodies or assays for palmitoylation detection. Acyl-biotin exchange assays are widely used, but as it detects palmitoylated proteins through detection of the palmitoyl–cysteinyl thioester linkage, any proteins or posttranslational modifications that utilize thioesters for chemistries other than palmitoylation may also be purified by this assay. The assay readout therefore potentially includes other types of lipid modifications, although palmitoylation is dominant. We noticed that Kir6.2-C166V mutation was still marginally detectible with this assay (Fig. 3*B*), which may represent another thioester-mediated modification on Kir6.2, or possibly a stable form of palmitoylation at another cysteine residue that is not regulated by PA or ML.

SwissPalm is a web-based resource that lists identified and predicted palmitoylated proteins (47). Kir6.1, Kir6.2, and Kir3.4 (and most other ion channels shown experimentally to be palmitoylated) are not present in this database. A major limitation of the SwissPalm database, however, is that the majority of tissue and cell types represented (COS cells, HEK cells, B cells, yeast, and so forth) do not express K_{ATP} channels. In terms of tissue/cells that do express K_{ATP} channels, this database is particularly limited. Heart, for example, has a total of two hits in Release 3 (2019-09-08), whereas ventricular myocytes show one hit (a different protein), which is far fewer than the number of palmitoylated proteins identified experimentally in cardiac tissue. Thus, although useful in many cases, experimental approaches are needed to supplement this database.

Materials and Methods

cDNA Constructs and Mutagenesis. Tagged K_{ATP} channel subunit constructs used are Avi-Kir6.2, Kir6.2-myc, Flag-SUR1, and Flag-SUR2A. The Kir3.4 construct is a kind gift from D. Logothetis, Northeastern University Bouvé College of Health Sciences, Boston, MA. Kir6.2 mutations (C166V, C166F and C166Y) and Kir2.1 mutation (A178C) were performed commercially and sequenced (Genscript).

Cell Culture and Transfection. HEK-293 cells were cultured in EMEM with 10% FBS. Lipofectamine 2000 was used to transfect K_{ATP} channel subunit cDNAs. INS-1 rat insulin-secreting cells were cultured in RPMI-1640 supplemented with 10% FBS, 10 mM Hepes, 1 mM sodium pyruvate, and 0.05 mM 2-mercaptoethanol. Rat ventricular cardiomyocytes were enzymatically isolated as previously described (48). Cells were plated on laminin-coated coverslips and cultured in EMEM. To induce palmitoylation, HEK-293 and INS-1 cells were incubated for 24 h with either 10 μM palmitic acid or with 10 μM ML348 plus 10 μM ML349. Particularly, rat cardiomyocytes were treated with palmitate–albumin complex (49) (working concentrations are 500 μM palmitate and 125 μM albumin, at a ratio of 4), and same amount of albumin was applied in control and ML groups.

Electrophysiology. We performed inside-out K_{ATP} current patch-clamp recordings as previously described in our recent study (50). After baseline subtraction, channel openings were detected by event detection using Clampfit 10.5, with the threshold set to 50% of the unitary current amplitude. Events with a duration shorter than 0.15 ms were not included in analysis. Burst analysis was performed as described previously (51). In whole-cell K_{ATP} current recordings, the pipettes (2~3 MΩ) were filled with: 110 mM potassium aspartic acid, 10 mM KCl, 5 mM NaCl, 1 mM $MgCl_2$, 5 mM EGTA, 5 mM NaATP, 10 mM Hepes, and pH 7.2. The bath solution consisted of: 137 mM NaCl, 0.33 mM NaH_2PO_4, 5.4 mM KCl, 1 mM $CaCl_2$, 1 mM $MgCl_2$, 10 mM glucose, 10 mM Hepes, and pH 7.4. Whole-cell current–voltage relationships were obtained using a ramp protocol (−5 mV to −105 mV at $-25\ mV{\cdot}s^{-1}$, applied every 30 s).

Biotinylation Assay. HEK-293 cells expressing Avi-tagged Kir6.2 were incubated with 0.33 mM biotin for 1 h at 4 °C. After washing with PBS, cells were homogenized in RIPA buffer. Equal amounts of biotinylated proteins were incubated with Neutravidin agarose beads (Thermo Scientific) at 4 °C overnight. The supernatants were discarded and biotinylated proteins were eluted by a mixture of loading buffer and 200 mM DTT. Western blots were quantified using ImageJ.

Acyl-Biotin Exchange Assay. Acyl-biotin exchange assay was performed as previously described (14) with minor modifications. Briefly, cell lysate was prepared in lysis buffer (150 mM NaCl, 50 mM Tris, 5 mM EDTA, pH 7.4) with 10 mM *N*-ethylmaleimide, 1.7% Triton X-100, and protease inhibitors. After a brief low-speed centrifugation to remove particles and unbroken cells, 10% of the sample was kept as total lysate for Western blots. The remaining sample was chloroform–methanol-precipitated and redissolved in 300 μL 4% SDS buffer with 10 mM *N*-ethylmaleimide under 37 °C. After adding 900 μL lysis buffer with 1 mM *N*-ethylmaleimide, 0.2% Triton X-100, and protease inhibitors, samples were incubated overnight at 4 °C with gentle rocking. The next day, *N*-ethylmaleimide was removed by three sequential chloroform–methanol precipitation steps. The protein pellet was dissolved and divided into two equal groups. In one group, Cys-palmitoyl thioester linkages were cleaved with 700 mM hydroxylamine (NH_2OH), whereas the negative-control group used Tris instead. Any remaining chemicals were removed by one chloroform–methanol precipitation and exposed thiols of the resolubilized proteins were labeled with 200 μM biotin-HPDP (14). Biotinylated proteins in buffer with 0.1% SDS and 0.2% Triton X-100 were captured by streptavidin beads, washed four times by lysis buffer with 0.1% SDS and 0.2% Triton X-100, and subjected to SDS/PAGE.

Immunocytochemistry. As previously described (24), isolated rat cardiomyocytes were plated on glass coverslips and fixed with 4% paraformaldehyde. Cells were permeabilized with 0.1% Triton X-100 and blocked with 5% donkey serum in PBS. Kir6.2 and secondary antibodies buffered in blocking solution were sequentially applied. After washing and mounting, images were obtained by Zeiss 700 confocal microscope (Zeiss).

Antibodies. Primary antibodies used were: mouse anti-GAPDH (G8795, Sigma-Aldrich; 1:10,000), mouse anti-c-Myc (M4439, Sigma-Aldrich; 1:6,000), rabbit anti-Flag (F7425, Sigma; 1:4,000), mouse anti-HA (901502, Biolegend; 1:10,000), rabbit anti-Kir6.2 (Lee62; 1:1,000), and chicken anti-Kir6.2 (C62; 1:50). Secondary antibodies used were donkey anti-mouse-HRP (715-035-150, Jackson, 1:20,000), goat anti-rabbit HRP (65-6120, Thermo Scientific; 1:20,000), and donkey anti-chicken Alexa Fluor488 (703-545-155, Jackson Laboratories; 1:200).

Molecular Modeling. All molecular modeling, alignments, and computational simulations were performed with the Internal Coordinates Mechanics software, (ICM-Pro, Molsoft). For the open-conformation K_{ATP} channel homology model, zero-end gap global sequence alignment between the human Kir6.2 sequence (Uniprot: Q14654) and the Kir3.2 3D structure (PDB ID code 3SYQ) produced a *P* value of 10^{-32} for 3D structural similarity. In prior work, precise homology modeling produces 3D structural models of equivalent accuracy

to the experimental template structure (3.44 Å) when the *P* value is so low (52). A homology model of the human Kir6.2 channel was thus built as previously described (53), by using PDB ID code 3SYQ as a structural template. For the closed conformation of K_{ATP} channel, we used PDB ID code 6C3P, which was resolved by cryo-EM at 5.6 Å, as the starting point for a 3D model. Missing side chains were built into the model, followed by biased probability Monte Carlo energy minimization in order to optimize the structure (54). For point mutations, individual models exhibiting palmiotylation or mutations of cysteine-166 (Cys^{166}) were generated using the "modify" command in ICM-Pro, which replaces, in the open-conformation homology model or the closed-conformation refined model, a specified side-chain atom group and bonding pattern (in this case Cys^{166}) with the side chain atoms and bonding pattern of a different specified amino acid. The newly introduced side chain, neighboring side chains, and the local backbone are then all subjected to Monte Carlo energy minimization as a single ensemble.

Statistics. When comparing two groups, we used the Student's *t* test. A one-way or two-way ANOVA was used for comparison of multiple groups, followed by the Dunnett's *t* test for comparisons to a single control. A value of $P < 0.05$ was considered significant. The statistical model underlying the homology modeling alignments has previously been described (52).

Data Availability Statement. All relevant material is contained within the main text or *SI Appendix*.

ACKNOWLEDGMENTS. This work was supported by NIH Grants HL126905 (to W.A.C.), HL146514 (to W.A.C.), S10 OD021589 (to W.A.C.), F31-HL124898-04 (to W.M.-O.), and an American Heart Association Grant 17POST33370050 (to H.-Q.Y.).

1. D. T. Lin, E. Conibear, Enzymatic protein depalmitoylation by acyl protein thioesterases. *Biochem. Soc. Trans.* **43**, 193–198 (2015).
2. D. T. Lin, E. Conibear, ABHD17 proteins are novel protein depalmitoylases that regulate N-Ras palmitate turnover and subcellular localization. *eLife* **4**, e11306 (2015).
3. A. D. Cox, C. J. Der, M. R. Philips, Targeting RAS membrane association: Back to the future for anti-RAS drug discovery? *Clin. Cancer Res.* **21**, 1819–1827 (2015).
4. C. Aicart-Ramos, R. A. Valero, I. Rodriguez-Crespo, Protein palmitoylation and subcellular trafficking. *Biochim. Biophys. Acta* **1808**, 2981–2994 (2011).
5. E. Tortosa, C. C. Hoogenraad, Polarized trafficking: The palmitoylation cycle distributes cytoplasmic proteins to distinct neuronal compartments. *Curr. Opin. Cell Biol.* **50**, 64–71 (2018).
6. M. N. Foster, W. A. Coetzee, KATP channels in the cardiovascular system. *Physiol. Rev.* **96**, 177–252 (2016).
7. M. J. Shipston, Ion channel regulation by protein S-acylation. *J. Gen. Physiol.* **143**, 659–678 (2014).
8. A. Tinker, Q. Aziz, Y. Li, M. Specterman, ATP-sensitive potassium channels and their physiological and pathophysiological roles. *Compr. Physiol.* **8**, 1463–1511 (2018).
9. E. Shumilina *et al*., Cytoplasmic accumulation of long-chain coenzyme A esters activates KATP and inhibits Kir2.1 channels. *J. Physiol.* **575**, 433–442 (2006).
10. D. Schulze, M. Rapedius, T. Krauter, T. Baukrowitz, Long-chain acyl-CoA esters and phosphatidylinositol phosphates modulate ATP inhibition of KATP channels by the same mechanism. *J. Physiol.* **552**, 357–367 (2003).
11. M. D. Resh, Use of analogs and inhibitors to study the functional significance of protein palmitoylation. *Methods* **40**, 191–197 (2006).
12. Z. Pei, Y. Xiao, J. Meng, A. Hudmon, T. R. Cummins, Cardiac sodium channel palmitoylation regulates channel availability and myocyte excitability with implications for arrhythmia generation. *Nat. Commun.* **7**, 12035 (2016).
13. S. J. Won *et al*., Molecular mechanism for isoform-selective inhibition of acyl protein thioesterases 1 and 2 (APT1 and APT2). *ACS Chem. Biol.* **11**, 3374–3382 (2016).
14. J. Wan, A. F. Roth, A. O. Bailey, N. G. Davis, Palmitoylated proteins: Purification and identification. *Nat. Protoc.* **2**, 1573–1584 (2007).
15. K. R. Tonn Eisinger *et al*., Palmitoylation of caveolin-1 is regulated by the same DHHC acyltransferases that modify steroid hormone receptors. *J. Biol. Chem.* **293**, 15901–15911 (2018).
16. N. Zerangue, B. Schwappach, Y. N. Jan, L. Y. Jan, A new ER trafficking signal regulates the subunit stoichiometry of plasma membrane K(ATP) channels. *Neuron* **22**, 537–548 (1999).
17. R. Bränström *et al*., Single residue (K332A) substitution in Kir6.2 abolishes the stimulatory effect of long-chain acyl-CoA esters: Indications for a long-chain acyl-CoA ester binding motif. *Diabetologia* **50**, 1670–1677 (2007).
18. N. Li *et al*., Structure of a pancreatic ATP-sensitive potassium channel. *Cell* **168**, 101–110.e10 (2017).
19. M. S. Rana *et al*., Fatty acyl recognition and transfer by an integral membrane *S*-acyltransferase. *Science* **359**, eaao6326 (2018).
20. K. Lemonidis *et al*., Substrate selectivity in the zDHHC family of *S*-acyltransferases. *Biochem. Soc. Trans.* **45**, 751–758 (2017).
21. R. N. P. Rodenburg *et al*., Stochastic palmitoylation of accessible cysteines in membrane proteins revealed by native mass spectrometry. *Nat. Commun.* **8**, 1280 (2017).
22. R. Stix, J. Song, A. Banerjee, J. D. Faraldo-Gomez, DHHC20 palmitoyl-transferase reshapes the membrane to foster catalysis. *Biophys. J.* **118**, 980–988 (2019).
23. S. Trapp, P. Proks, S. J. Tucker, F. M. Ashcroft, Molecular analysis of ATP-sensitive K channel gating and implications for channel inhibition by ATP. *J. Gen. Physiol.* **112**, 333–349 (1998).
24. H. Q. Yang, K. Jana, M. J. Rindler, W. A. Coetzee, The trafficking protein, EHD2, positively regulates cardiac sarcolemmal K_{ATP} channel surface expression: Role in cardioprotection. *FASEB J.* **32**, 1613–1625 (2018).
25. D. W. Hilgemann, R. Ball, Regulation of cardiac Na+,Ca2+ exchange and KATP potassium channels by PIP2. *Science* **273**, 956–959 (1996).
26. L. H. Xie, M. Takano, M. Kakei, M. Okamura, A. Noma, Wortmannin, an inhibitor of phosphatidylinositol kinases, blocks the MgATP-dependent recovery of Kir6.2/SUR2A channels. *J. Physiol.* **514**, 655–665 (1999).
27. L. H. Xie, M. Horie, M. Takano, Phospholipase C-linked receptors regulate the ATP-sensitive potassium channel by means of phosphatidylinositol 4,5-bisphosphate metabolism. *Proc. Natl. Acad. Sci. U.S.A.* **96**, 15292–15297 (1999).
28. S. L. Shyng, C. G. Nichols, Membrane phospholipid control of nucleotide sensitivity of K_{ATP} channels. *Science* **282**, 1138–1141 (1998).
29. M. J. Berridge, Inositol trisphosphate and calcium signalling. *Nature* **361**, 315–325 (1993).
30. H. W. De Jonge, H. A. Van Heugten, J. M. Lamers, Signal transduction by the phosphatidylinositol cycle in myocardium. *J. Mol. Cell. Cardiol.* **27**, 93–106 (1995).
31. M. Horie, M. Tei, C. Kawai, H. Irisawa, Effect of alpha-1-adrenergic agonists on inwardly rectifying background K+ currents (IK1) in single Guinea pig heart cells. *Jpn. Circ. J.* **52**, 990 (1988).
32. D. Fedida, A. P. Braun, W. R. Giles, Alpha 1-adrenoceptors reduce background K+ current in rabbit ventricular myocytes. *J. Physiol.* **441**, 673–684 (1991).
33. S. Kobayashi *et al*., Endothelin-1 partially inhibits ATP-sensitive K+ current in Guinea pig ventricular cells. *J. Cardiovasc. Pharmacol.* **27**, 12–19 (1996).
34. T. Haruna *et al*., Alpha1-adrenoceptor-mediated breakdown of phosphatidylinositol 4,5-bisphosphate inhibits pinacidil-activated ATP-sensitive K+ currents in rat ventricular myocytes. *Circ. Res.* **91**, 232–239 (2002).
35. C. G. Nichols, K_{ATP} channels as molecular sensors of cellular metabolism. *Nature* **440**, 470–476 (2006).
36. M. R. Whorton, R. MacKinnon, Crystal structure of the mammalian GIRK2 K+ channel and gating regulation by G proteins, PIP2, and sodium. *Cell* **147** (1):), 199–208, 10.1016/j.cell.2011.07.046 (2011).
37. K. P. K. Lee, J. Chen, R. MacKinnon, Molecular structure of human KATP in complex with ATP and ADP. *Elife* **6**, 10.7554/eLife.32481 (2017).
38. W. Martinez-Ortiz, T. J. Cardozo, An improved method for modeling voltage-gated ion channels at atomic accuracy applied to human Ca_v channels. *Cell Rep.* **23**, 1399–1408 (2018).
39. R. A. Gubitosi-Klug, D. J. Mancuso, R. W. Gross, The human Kv1.1 channel is palmitoylated, modulating voltage sensing: Identification of a palmitoylation consensus sequence. *Proc. Natl. Acad. Sci. U.S.A.* **102**, 5964–5968 (2005).
40. X. Y. Meng, S. Liu, M. Cui, R. Zhou, D. E. Logothetis, The molecular mechanism of opening the helix bundle crossing (HBC) gate of a Kir channel. *Sci. Rep.* **6**, 29399 (2016).
41. B. C. Suh, D. I. Kim, B. H. Falkenburger, B. Hille, Membrane-localized β-subunits alter the PIP2 regulation of high-voltage activated Ca2+ channels. *Proc. Natl. Acad. Sci. U.S.A.* **109**, 3161–3166 (2012).
42. L. Reilly *et al*., Palmitoylation of the Na/Ca exchanger cytoplasmic loop controls its inactivation and internalization during stress signaling. *FASEB J.* **29**, 4532–4543 (2015).
43. S. L. Shyng, C. A. Cukras, J. Harwood, C. G. Nichols, Structural determinants of PIP(2) regulation of inward rectifier K(ATP) channels. *J. Gen. Physiol.* **116**, 599–608 (2000).
44. D. W. Hilgemann *et al*., Lipid signaling to membrane proteins: From second messengers to membrane domains and adapter-free endocytosis. *J. Gen. Physiol.* **150**, 211–224 (2018).
45. Y. P. Zhou, V. E. Grill, Long-term exposure of rat pancreatic islets to fatty acids inhibits glucose-induced insulin secretion and biosynthesis through a glucose fatty acid cycle. *J. Clin. Invest.* **93**, 870–876 (1994).
46. P. E. Cooper *et al*., Cantú syndrome resulting from activating mutation in the KCNJ8 gene. *Hum. Mutat.* **35**, 809–813 (2014).
47. M. Blanc *et al*., SwissPalm: Protein palmitoylation database. *F1000 Res.* **4**, 261 (2015).
48. M. Hong *et al*., Cardiac ATP-sensitive K^+ channel associates with the glycolytic enzyme complex. *FASEB J.* **25**, 2456–2467 (2011).
49. A. F. Oliveira *et al*., In vitro use of free fatty acids bound to albumin: A comparison of protocols. *Biotechniques* **58**, 228–233 (2015).
50. H. Q. Yang *et al*., Ankyrin-G mediates targeting of both Na^+ and K_{ATP} channels to the rat cardiac intercalated disc. *eLife* **9**, e52373 (2020).
51. K. L. Magleby, B. S. Pallotta, Burst kinetics of single calcium-activated potassium channels in cultured rat muscle. *J. Physiol.* **344**, 605–623 (1983).
52. R. A. Abagyan, S. Batalov, Do aligned sequences share the same fold? *J. Mol. Biol.* **273**, 355–368 (1997).
53. T. Cardozo, M. Totrov, R. Abagyan, Homology modeling by the ICM method. *Proteins* **23**, 403–414 (1995).
54. R. Abagyan, M. Totrov, Biased probability Monte Carlo conformational searches and electrostatic calculations for peptides and proteins. *J. Mol. Biol.* **235**, 983–1002 (1994).